Graphical analysis of the orthopyroxene-pigeonite-augite-plagioclase equilibrium at liquidus temperatures and low pressure

Article *in* American Mineralogist · April 2001

DOI: 10.2138/am-2001-0417

CITATIONS
6

READS
141

4 authors, including:

Rais Latypov
University of the Witwatersrand
107 PUBLICATIONS **1,009** CITATIONS

SEE PROFILE

American Mineralogist, Volume 86, pages 547–554, 2001

Graphical analysis of the orthopyroxene-pigeonite-augite-plagioclase equilibrium at liquidus temperatures and low pressure

RAIS M. LATYPOV,[1,*] MICHAIL I. DUBROVSKII,[1] AND TUOMO T. ALAPIETI[2]

[1] Geological Institute, Kola Science Centre, Apatity, 184200, Russia
[2] Institute of Geosciences, University of Oulu, FIN–90014, Finland

ABSTRACT

There are both natural and experimental observations of the coexistence of three pyroxenes—orthopyroxene (Opx) + pigeonite (Pig) + augite (Aug)—with plagioclase (Pl). Commonly, the assemblage occurs as an intermediate product in the following fractionation trend of a mafic magma: Opx + Aug + Pl → Opx + Aug + Pig + Pl → Aug + Pig + Pl. To clarify the phase-equilibria constraints on the existence of this mineral assemblage, we have graphically analyzed the change in topology of an isobaric–isoplethic section, Ol-Aug-Pl-Qtz [with *fe* = 25–50%, where *fe* = Fe/(Fe + Mg), and An = 50%], arising from an increase in the *fe*-value of silicate liquid. The analysis shows that the stability field of the mineral assemblage Opx + Aug + Pig + Pl is restricted, and can only crystallize in the interval between two invariant points—T_1^4(Ol + Opx + Pig + Aug + Pl + L) and T_2^4(Qtz + Opx + Pig + Aug + Pl + L)—that emerge successively during expansion of a liquidus volume of pigeonite within the isobaric–isoplethic section Ol-Aug-Pl-Qtz. At *fe*-values lower than T_1^4, the 3-pyroxene assemblage cannot exist due to the absence of a contact surface between the primary volumes of plagioclase and pigeonite. At *fe*-values greater than T_2^4, the assemblage is unstable due to separation of the primary volumes of orthopyroxene and augite.

INTRODUCTION

The coexistence of three pyroxenes, orthopyroxene (Opx)[1] + pigeonite (Pig) + augite (Aug), with plagioclase (Pl) is not very common in nature. However, the assemblage develops in differentiating andesitic and basaltic magmas during a brief period of peritectic replacement of Opx by Pig. Among effusive rocks, perhaps the best example of a three-pyroxene paragenesis is in the andesites of Weiselberg, Germany (Nakamura and Kushiro 1970). During fractional crystallization of those magmas, the phenocryst assemblage changed from Aug + Opx + Pl through Aug + Opx + Pig + Pl to Aug + Pig + Pl, coincident with an increasing Fe/Mg ratio. Among plutonic rocks, the transition from an Aug + Opx + Pl assemblage to one containing Aug + Pig + Pl—occurring through the period of simultaneous crystallization of three pyroxenes and plagioclase—is most pronounced in the Bushveld Complex. There, the three-pyroxene paragenesis is found throughout ~1 Km of the central part of the Main Zone of the Complex (Von Gruenewaldt 1970; Eales and Cawthorn 1996). The first author of the present paper observed a three-pyroxene assemblage during an investigation of magnetite gabbro of the West Pansky Tundra layered intrusion, Russia (Latypov and Chistyakova 2001). Layers and lenticular bodies of magnetite gabbro, considered to be a late-stage product of differentiation in the magma chamber, are prominent in the gabbronorite zone of the intrusion (Odinets 1971; Kozlov 1973). The transition from the host gabbronorites to magnetite gabbro is characterized by the mineral sequence: Pl + Opx + Aug (gabbronorite) → Pl + Aug + Opx + Pig (gabbro with inverted pigeonite) → Pl + Aug + Opx + Pig + Mgt (magnetite gabbro with inverted pigeonite) (Latypov and Chistyakova 2001).

Experimental investigations of the stability relations of Aug, Opx, and Pig in Fe-bearing systems (Huebner and Turnock 1980) made it possible at the beginning of the 1990s to construct tentative phase diagrams showing shifts in the pyroxene liquidus boundaries of a basaltic melt (Longhi and Pan 1988; Longhi 1991). However, due to numerous difficulties discussed by Longhi and Pan (1988) and Longhi (1991), the stability relations of the Opx + Pig + Aug + Pl assemblage could not be determined adequately. The main aim of the present paper is to address this issue by clarifying the liquidus phase relations using a qualitative approach. No attempts have been made to estimate the temperatures of the phase equilibria, due to absence of constraining results from field and laboratory studies performed to date.

* E-mail: rais.latypov@oulu.fi

[1]Hereinafter: Ol = olivine, Aug = augite, Pl = plagioclase, Qtz = quartz, Opx = orthopyroxene, Pig = pigeonite, Fo = forsterite, Fa = fayalite, Di = diopside, Hd = hedenbergite, An = anorthite, Ab = albite, En = enstatite, Pr = proroenstatite, Sp = spinel, L = liquid. E = eutectic equilibrium, P = peritectic equilibrium, S = singular equilibriium, T = 6-phase invariant equilibrium. $Ol^{25\text{-}50}$ = olivine with *fe* = 25–50% [where *fe* = Fe/(Fe + Mg)], Pl^{60} = plagioclase with An = 60%.

PHASE EQUILIBRIA DIAGRAMS

Geometrical analysis of the changes in the topologies of the phase diagrams with an increase in *fe* ratio of the melt was performed using the isobaric–isoplethic section Ol^{25-50}-Aug-Pl^{60}-Qtz in the 6-component system Fo-Fa-Di-Hd-Ab-An-Qtz (Fig. 1). This section has been slightly modified from Dubrovskii (1998) by applying the standard approach for graphical analysis of phase equilibria, described in the works of Schreinemakers (1965), Ricci (1951), Korzhinskii (1959), and Ehlers (1972). The choice of an isobaric–isoplethic section is prompted by appearance of pigeonite on the liquidus in basaltic magmas at Fe/Mg = 30/70 (Hess 1941), which is within the compositional range of the section. The silica-saturation plane, Opx-Aug-Pl, separates the Ol-Aug-Pl-Qtz tetrahedron into two isoplethic sections: a quartz-normative section, Opx-Aug-Pl-Qtz, and an olivine-normative section, Ol-Opx-Aug-Pl. The system also contains two isobaric invariant points: eutectic point E_1^4, Qtz + Opx + Aug + P = L, and tributary point P_1^4, Opx + Aug + Pl = L + Ol.

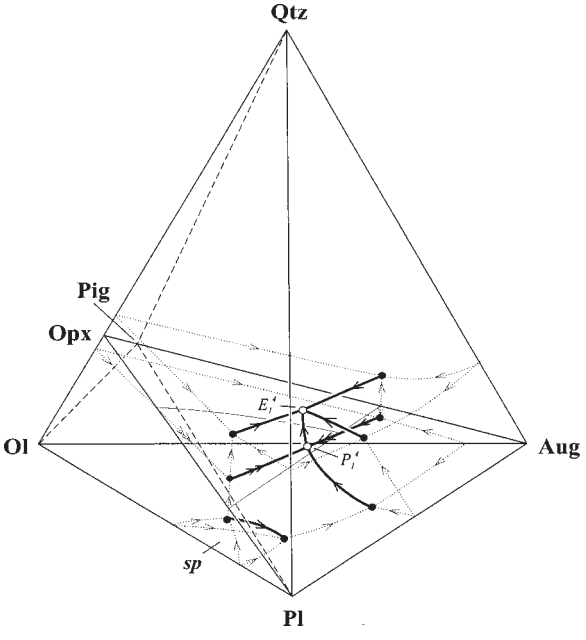

FIGURE 1. Phase relations along the isobaric–isoplethic section Ol^{25-50}-Aug-Pl^{60}-Qtz at P < 1000 bar, with compositions of the components expressed in wt% (slightly modified from Dubrovskii 1998). Thick solid curves indicate liquidus lines within the Ol-Aug-Pl-Qtz tetrahedron; dotted curves are liquidus lines on the faces of the tetrahedron. Invariant points in the interior of the tetrahedron are shown as open circles. Filled circles represent ternary points on the faces of the tetrahedron. Two solid, fine lines illustrate the intersection of the divariant surfaces Ol-Opx-L, Ol-Pl-L, Ol-Aug-L, and Opx-Aug-L with the silica-saturation plane Opx-Aug-Pl. Hereafter, cotectic and reaction lines are indicated by one and two arrows, respectively. Reactions and phase assemblages depicted in Figures 1–7 are listed in Table 1. Arrows point toward decreasing temperature. For clarity, a eutectic point on the Qtz-Pl join is displaced slightly from its true position, toward the Pl apex.

CONSTRAINTS PROVIDED BY EXPERIMENTAL WORK

Yang (1973) and Longhi (1987) have shown that progressive expansion of the primary crystallization volume of Fe-free pigeonite in the tetrahedron Fo-Di-An-Qtz, and the volume of Fe-rich pigeonite in the tetrahedron Ol-Aug-Pl-Qtz (Longhi and Pan 1988; Longhi 1991), takes place from the boundary face Ol-Aug-Qtz (or Fo-Di-Qtz) toward the inside of the tetrahedron. In principal, the expansion can be illustrated within the volume of a tetrahedron; however, the resulting diagram is very complicated. A more effective means of illustration is to display the primary volume of pigeonite in an enlarged plot of the central portion of the tetrahedron. This is done in Figure 2, which is a magnified part of the phase diagram constructed by Yang (1973, see his Fig. 1). Note that the primary volume of Fe-free pigeonite is separated from the one for anorthite. A quaternary isobaric invariant point P_2^4 (Fo + Pig + Pr + Di + L; point f in Yang 1973) is proposed on the basis of the following order of phase crystallization: Fo + L (1–2) → Fo + Pr + L (2–3) → Fo + Pr + Pig + L (3–4) → Fo + Pr + Pig + Di + L (4) → Fo + Pr + Di + L (4–5) (Fig. 2). The existence of another invariant point, P_3^4, Qtz + Pig + Pr + Di + L, also has been suggested (point e; Fig. 1 in Yang 1973), but not verified experimentally.

Grove and Juster (1989) performed experiments to determine the stability of low-Ca pyroxene at 1 atm in natural basaltic and andesitic liquids. Two trends of crystallization within the Medicine Lake andesites, California, are relevant to the present discussion. These are Trend I, Ol + Pl + L (1) → Ol + Pl + Pig + Aug + L (2) → Pl + Pig + Aug + L (3) → Pl + Pig + Aug + Opx + L (4) (sample 79–38b); and Trend II, Ol + Pl + L (1) → Ol + Pl + Opx + L (2) → Ol + Pl + Opx + Pig + L (3) → Pl + Pig + L (4) → Pl + Pig + Aug + Opx + L (5) (sample 38b–8a). (Grove and Juster 1989, their Fig. 2, Table 2). Both trends are characterized by the mineral assemblage Pl + Pig + Aug + Opx as the final product of crystallization. A distinguishing feature of the second trend is the existence of an intermediate assemblage in which orthopyroxene is absent. The relevant

TABLE 1. Reactions and phase assemblages illustrated in Figures 1–7

Notation	Phase equilibria
E_1^4	Qtz + Opx + Aug + Pl = L
E_2^4	Qtz + Pig + Aug + Pl = L
E_3^4	Qtz + Opx + Pig + Pl = L
P_1^4	Opx + Aug + Pl = L + Ol
*P_2^4	Opx + Aug = L + Ol + Pig
*P_3^4	Qtz + Opx + Aug = L + Pig
P_4^4	Pig + Pl = L + Ol + Opx
P_5^4	Pig + Aug + Pl = L + Ol
P_6^4	Opx + Aug = L + Pig + Pl
P_7^4	Qtz + Pig + Pl = L + Opx
P_8^4	Opx + Pig + Pl = L + Ol
E_1^3	Opx + Aug + Pl = L
E_2^3	Pig + Aug + Pl = L
P_1^3	Opx + Aug = L + Pig
P_2^3	Pig + Pl = L + Opx
S_1^4	Ol + Opx + Pig + Pl + L
S_2^4	Qtz + Opx + Pig + Pl + L
T_1^4	Ol + Opx + Pig + Aug + Pl + L
T_2^4	Qtz + Opx + Pig + Aug + Pl + L
T^3	Opx + Aug + Pig + Pl + L

* In Figure 2, Di = Aug and Pr = Opx.

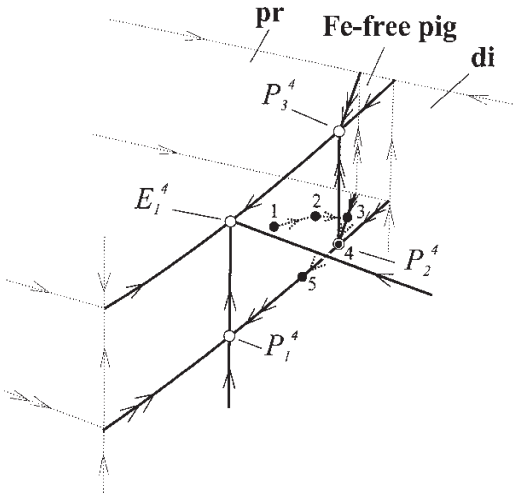

FIGURE 2. Liquidus phase relations in the interior of the tetrahedron Fo-Di-An-Qtz at atmospheric pressure (modified from Yang 1973). An experimentally determined trend of crystallization (from point 1 to point 5; Yang 1973), suggesting the occurrence of an isobaric invariant point P_2^4 in this system, is also shown. Hereafter, fine dotted lines in the front and back of a diagram are located on the Ol-Pl-Qtz and Ol-Aug-Qtz faces, respectively.

liquidus phase relations within the tetrahedron can be derived from the two trends of crystallization. They are depicted in Figure 3 in the form of volumetric isobaric–isoplethic sections.

Trend I (Fig. 3a)

Crystallization of the liquid starts at the divariant surface Ol + Pl + L (point 1) as crystallization proceeds; the composition of the liquid moves toward the distributary point Pig + Aug + Pl = L + Ol (P_5^4, point 2). Here, all olivine is exhausted, whereupon the liquid—by gaining an additional degree of freedom—subsequently travels along the univariant cotectic line Pig + Aug + Pl = L (path from point 2 to point 3). Upon further crystallization, the liquid reaches a distributary point Opx + Aug = L + Pig + Pl (P_6^4, point 4) where a new phase, orthopyroxene, is produced.

Trend II (Fig. 3b)

In this trend, crystallization of the liquid also starts from the divariant surface Ol + Pl + L (point 1), but thereafter the composition of the liquid moves along a univariant peritectic line Pl + Opx = L + Ol (point 2). With further cooling, the liquid reaches the distributary point Pig + Pl = L + Ol + Opx (P_4^4, point 3). There, olivine and orthopyroxene are consumed simultaneously; thus, the liquid gains two degrees of freedom, and its composition shifts to the divariant cotectic surface Pig + Pl = L (point 4 is located on this surface). With continued crystallization, the liquid reaches the distributary point Opx + Aug = L + Pig + Pl (P_6^4, point 5), where orthopyroxene appears in the phase assemblage along with augite.

Thus, the experimental results of Grove and Juster (1989) clearly show that further expansion of the pigeonite volume with increasing *fe*-value of the melt leads at some stage to three new invariant points: distributary point P_4^4, tributary point P_5^4, and distributary point P_6^4. This result suggests that the system must first pass through the invariant equilibrium Ol + Opx + Pig + Aug + Pl + L, which arises due to convergence of the isobaric invariant points P_1^4 and P_2^4 shown in Figure 2. Shi and Libourel (1991, their Fig. 1) predicted this 6-phase invariant equilibrium on the basis of Schreinemakers rules for the system CMAS + FeO. However, its existence has not yet been verified experimentally.

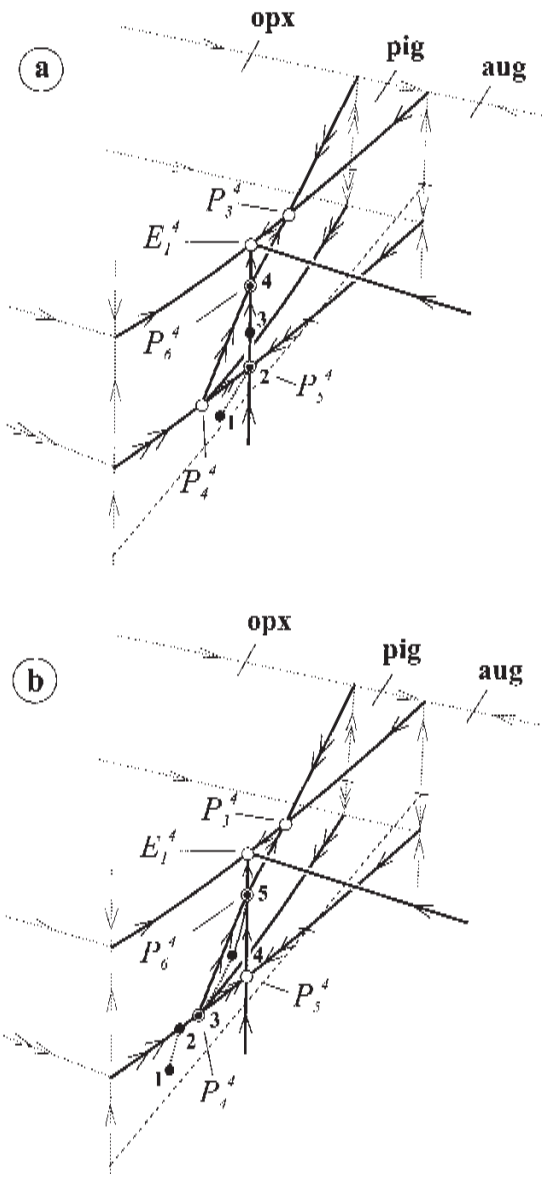

FIGURE 3. Liquidus phase relations in the interior of the tetrahedron Ol-Aug-Pl-Qtz at atmospheric pressure, based on the experimental data of Grove and Juster (1989). Two experimentally determined crystallization trends (a and b) of natural andesitic liquids (Grove and Juster 1989), indicating the existence of three isobaric invariant points P_3^4, P_4^4, and P_6^4 in the system, are shown. Dashed lines depict the position of the silica-saturation plane Opx-Aug-Pl.

Grove et al. (1982, 1983) provide insight into additional

changes in the topology of the phase diagram Ol-Aug-Pl-Qtz that occur with an increase in the *fe*-value of the melt. They constructed the diagram displayed in Figure 4a by projecting the compositions of basaltic and andesitic liquids from the pseudoquaternary system Ol-Aug-Pl-Qtz onto the boundary face Ol-Aug-Qtz. Applying the phase-equilibrium data of Grove et al. (1982, 1983), we have graphically constructed the relevant configuration of liquidus phase relations in the interior of the tetrahedron Ol-Aug-Pl-Qtz. Results are shown in Figure 4b. In that diagram, the univariant line Ol + Pig + Pl + L has a thermal maximum, TD, produced by the intersection of the line with an extension of the plane Ol-Pig-Pl (see Fig. 1). From topological analysis, it seems likely that a second thermal maximum, TD', is located on the univariant line Qtz + Pig + Pl + L (Fig. 4), which arises from intersection of the line with the plane Qtz + Pig + Pl (see Fig. 1).

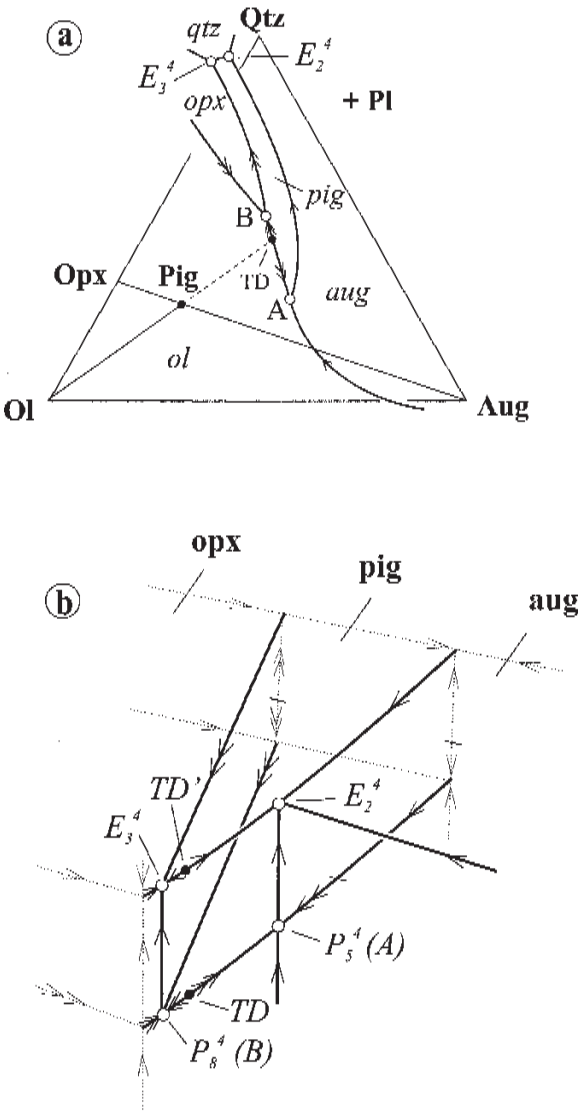

FIGURE 4. Projections of 1 atm liquidus phase relations in the tetrahedron Ol-Aug-Pl-Qtz onto the Ol-Aug-Qtz face: (**a**) Grove et al. (1983) (in oxygen units) and (**b**) this study (in wt%). TD is a thermal maximum formed by the intersection of the univariant line Ol + Pig + Pl + L with an extension of the plane Ol-Pig-Pl (Fig. 1). TD' is an assumed thermal maximum formed by the intersection of the univariant line Qtz + Pig + Pl + L with an extension of the plane Qtz-Pig-Pl (Fig. 1). The system contains four isobaric invariant points: P_5^4 (point A in Fig. 2 in Grove et al. 1983), P_8^4 (point B in Fig. 2 in Grove et al. 1983), E_2^4, and E_3^4.

To develop the topology of the phase diagram (Fig. 4b) containing the tributary point P_8^4 and the eutectic point E_3^4, the primary volume of pigeonite must expand in the tetrahedron and closely approach the boundary plane Ol + Pl + Qtz. From this observation, it follows that phase relations in the system must include the six-phase invariant equilibrium Qtz + Opx + Pig + Aug + Pl + L. This assemblage forms as a result of convergence of the distributary point P_6^4, the tributary point P_3^4, and the eutectic point E_1^4 (Fig. 3).

GRAPHICAL ANALYSIS OF PHASE EQUILIBRIA IN THE ISOBARIC-ISOPLETHIC SECTION $Ol^{25\text{-}50}$-Aug-Pl^{60}-Qtz WITH INCREASING *Fe*-VALUE

Using constraints imposed by experimental data (Yang 1973; Longhi 1987, 1991; Longhi and Pan 1988; Grove and Juster 1989; Grove et al. 1982, 1983; Shi and Libourel 1991), we have graphed the complete set of isobaric–isoplethic sections that illustrate changes in liquidus boundaries with increasing *fe*-value of the melt (Fig. 5). Three of these diagrams (*fe*1, *fe*2, and *fe*6) in Figure 5 have already been presented and discussed above. The remaining sections (*fe*2, *fe*4, and *fe*5) in Figure 5 were derived using the rules of Schreinemakers (1965). The locations of these sections with respect to *fe*-value are indicated by dotted lines on the isobaric *T-fe* diagram shown in Figure 6.

As the volume of pigeonite expands inside the tetrahedron, two reaction points arise in which three pyroxenes coexist with either quartz (P_3^4) or olivine (P_2^4) (Fig. 5, *fe*1). Further evolution of the system brings it to the invariant equilibrium T_1^4 (Ol + Opx + Pig + Aug + Pl + L). By our analysis, this invariant equilibrium appears when the tributary point P_1^4 converges with the distributary point P_2^4 (Fig. 5, *fe*2). Following this convergence, three new invariant points form: distributary point P_4^4, tributary point P_5^4, and distributary point P_6^4 (Fig. 5, *fe*3). It is at the latter point (P_6^4, Opx + Aug = L + Pig + Pl) where coexistence of three pyroxenes with plagioclase first becomes possible. This mineral assemblage soon becomes unstable, however, due to the appearance of a second invariant equilibrium T_2^4, Qtz + Opx + Pig + Aug + Pl + L (Fig. 5, *fe*2 and Fig. 6), which leads to complete separation of the primary volumes of augite and orthopyroxene. The invariant equilibria T_2^4 is formed owing to convergence of the distributary point P_6^4, tributary point P_3^4, and the eutectic point E_1^4 (Fig. 5, *fe*4 and Fig. 6). With a further increase in the *fe*-value, the new tributary point P_7^4 and the eutectic point E_2^4 must appear (Fig. 5, *fe*5). At some time later, the points P_7^4 and P_4^4 must convert to eutectic point E_3^4 and tributary point P_8^4, respectively, through the singular equilibria S_1^4 and S_2^4 (Fig. 5, *fe*6 and Fig. 6). This occurs when points P_7^4 and P_4^4 cross the thermal divides Ol-Pig-Pl and Qtz + Pig + Pl. Further expansion of the pigeonite volume could theoretically cause the isobaric points E_3^4 and P_8^4 to disappear when

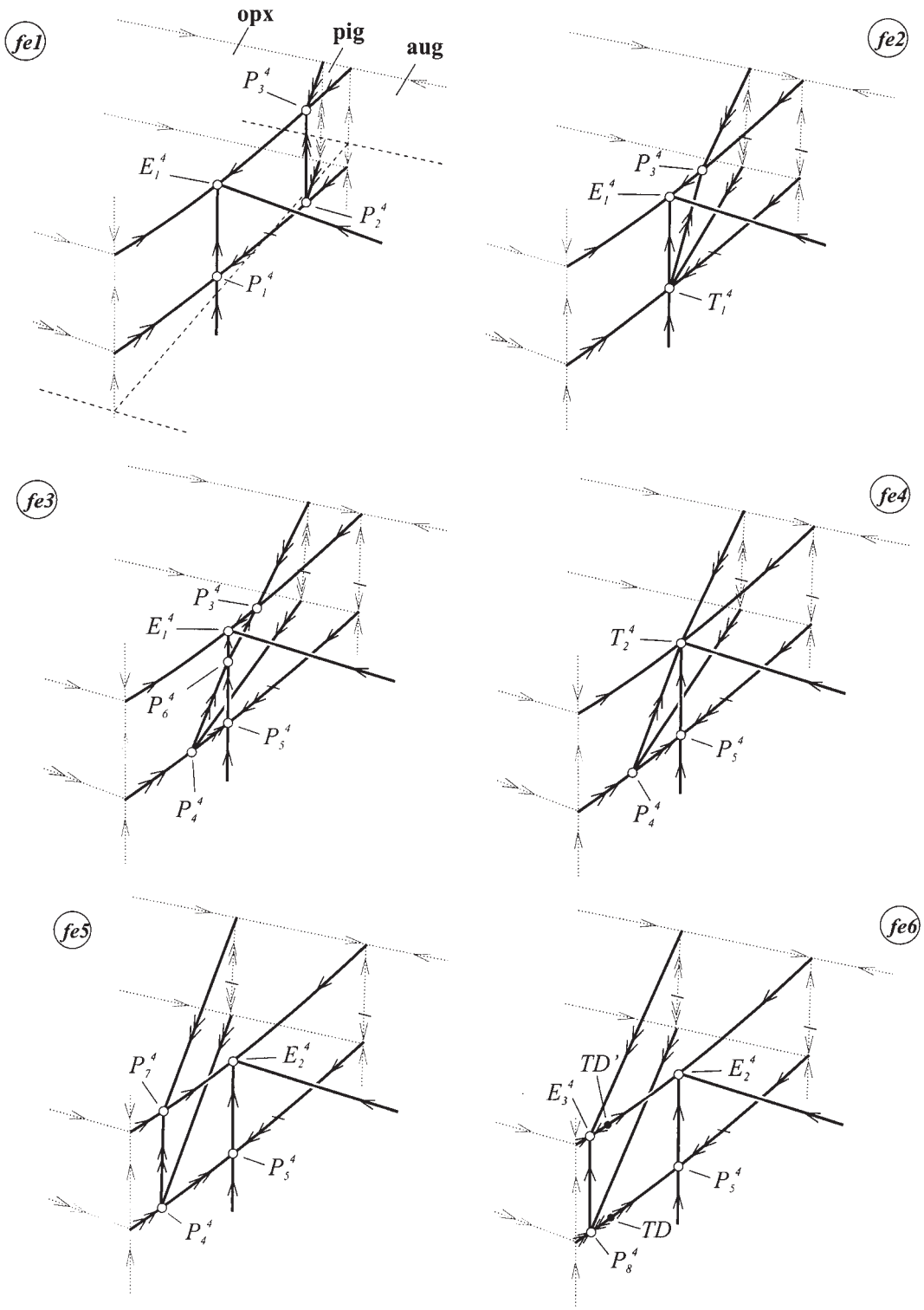

FIGURE 5. Systematic changes in the topologies of the isobaric–isoplethic sections Ol^{25-50}-Aug-Pl^{60}-Qtz due to an increase in the *fe*-value of the melt, which results in expansion of the primary pigeonite volume. The positions of the sections from *fe*1 to *fe*6 are indicated by dotted lines on the isobaric *T-fe* diagram (Fig. 6). In section *fe*1, dashed lines represent intersections of the univariant lines and surfaces with the silica-saturation plane Opx-Aug-Pl. In sections *fe*2 to *fe*6, the intersections are shown by short horizontal bars on univariant lines. Invariant points in the interior of the tetrahedron are shown as open circles.

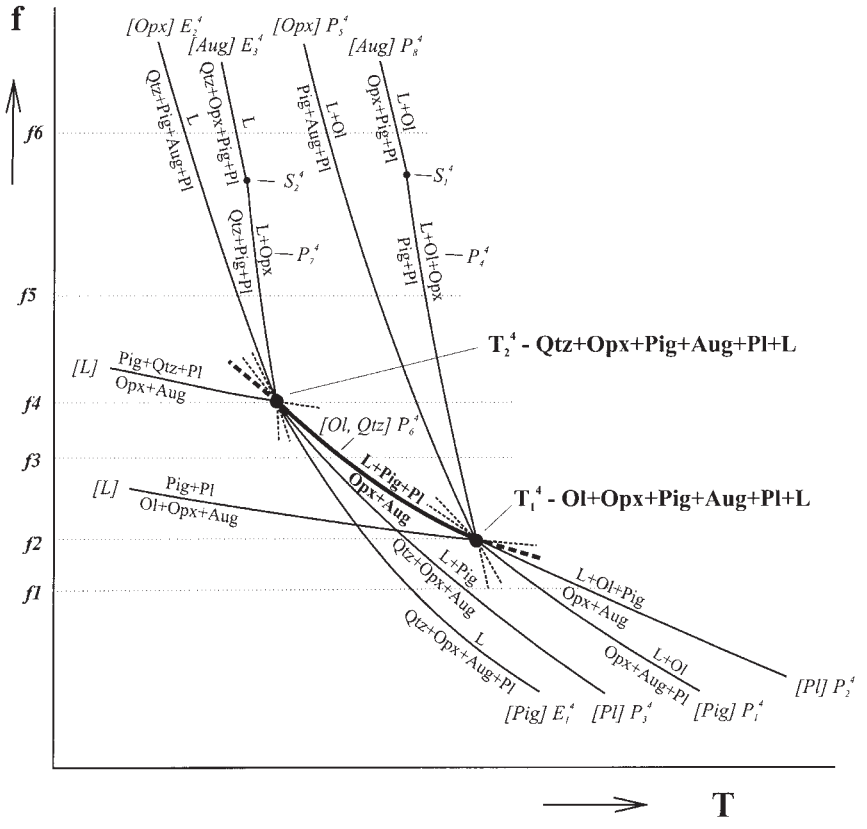

FIGURE 6. *T-fe* projection of the isobaric section $Ol^{25\text{-}50}$-Aug-P^{60}-Qtz. Dotted lines show the positions of the isobaric–isoplethic sections depicted in Figure 5. Brackets indicate phases that are absent in the equilibria.

they reach the Ol-Pl-Qtz boundary face. However, at present there is no experimental evidence that confirms this behavior.

Thus, the stability field of the mineral assemblage Opx + Aug + Pig + Pl in the isobaric–isoplethic section $Ol^{25–50}$-Aug-Pl^{60}-Qtz is restricted to a region between the invariant equilibria T_1^4 and T_2^4. At *fe*-values lower than that at T_1^4, this assemblage cannot form due to lack of contact surfaces between the primary volumes of plagioclase and pigeonite. At *fe*-values greater than that at T_2^4, the assemblage cannot exist owing to separation of the primary volumes of orthopyroxene and augite. The appearance of Opx + Aug + Pig + Pl in natural melts will depend greatly on the composition of the melt. Conditions that favor its appearance are a high concentration of An in normative plagioclase, and an *fe*-value that provides the greatest expansion of the primary volume of plagioclase and pigeonite (Longhi 1991). These circumstances lead to rapid convergence of the tributary point P_1^4 with the distributary point P_2^4 (invariant equilibrium T_1^4), after which the assemblage Opx + Aug + Pig + Pl + L forms (Fig. 5, P_6^4 in *fe*3). As an example, in two basalts with the same *fe*-value, this assemblage appears first in the basalt that contains a high concentration of An in normative plagioclase. Among two basalts with different *fe*-values, however, Opx + Aug + Pig + Pl does not necessarily form first in the basalt with the higher *fe*-value. The opposite may be true if the basalt with the lower *fe*-value contains the higher concentration of An in normative plagioclase.

IMPLICATIONS FOR THE PROBLEM OF CRYSTALLIZATION TRENDS OF MAFIC LAYERED INTRUSIONS

The rather complex topology of the phase relations (Fig. 5) that result from the occurrence of up to five isobaric points at various stages of crystallization permits a wide range of phase crystallization sequences involving three pyroxenes. Therefore, it is surprising that mafic layered intrusions do not display a wider variety of crystallization trends. Ignoring the highly Fe-rich late-stage products of differentiation of a mafic magma, most layered intrusions are characterized by the pyroxene crystallization sequence: Opx + Aug → Opx + Aug + Pig → Aug + Pig (Wager and Brown 1968). A reasonable explanation for this systematic trend is that crystallization of the parent magma of mafic/ultramafic intrusions reaches a gabbronorite cotectic line Opx + Aug + Pl = L before pigeonite appears on the liquidus. As a consequence, pyroxene-bearing assemblages can only form in a strictly specified order dictated by changes in the topology of the phase diagram Ol-Aug-Pl-Qtz that occur with the progressive expansion of the primary volume of pigeonite. This idea can be illustrated using isoplethic sections of the silica-saturation plane Opx + Aug + Pig (Fig. 7). In the course of fractional crystallization, the initial liquid X should eventually reach a gabbronorite eutectic E_1^3 (Fig. 7, *fe*1 and *fe*2), where it will start to precipitate the mineral assemblage Opx + Aug + Pl. The subsequent convergence of the peritectic and eutectic points P_1^3 and E_1^3, caused by expansion of the pigeonite

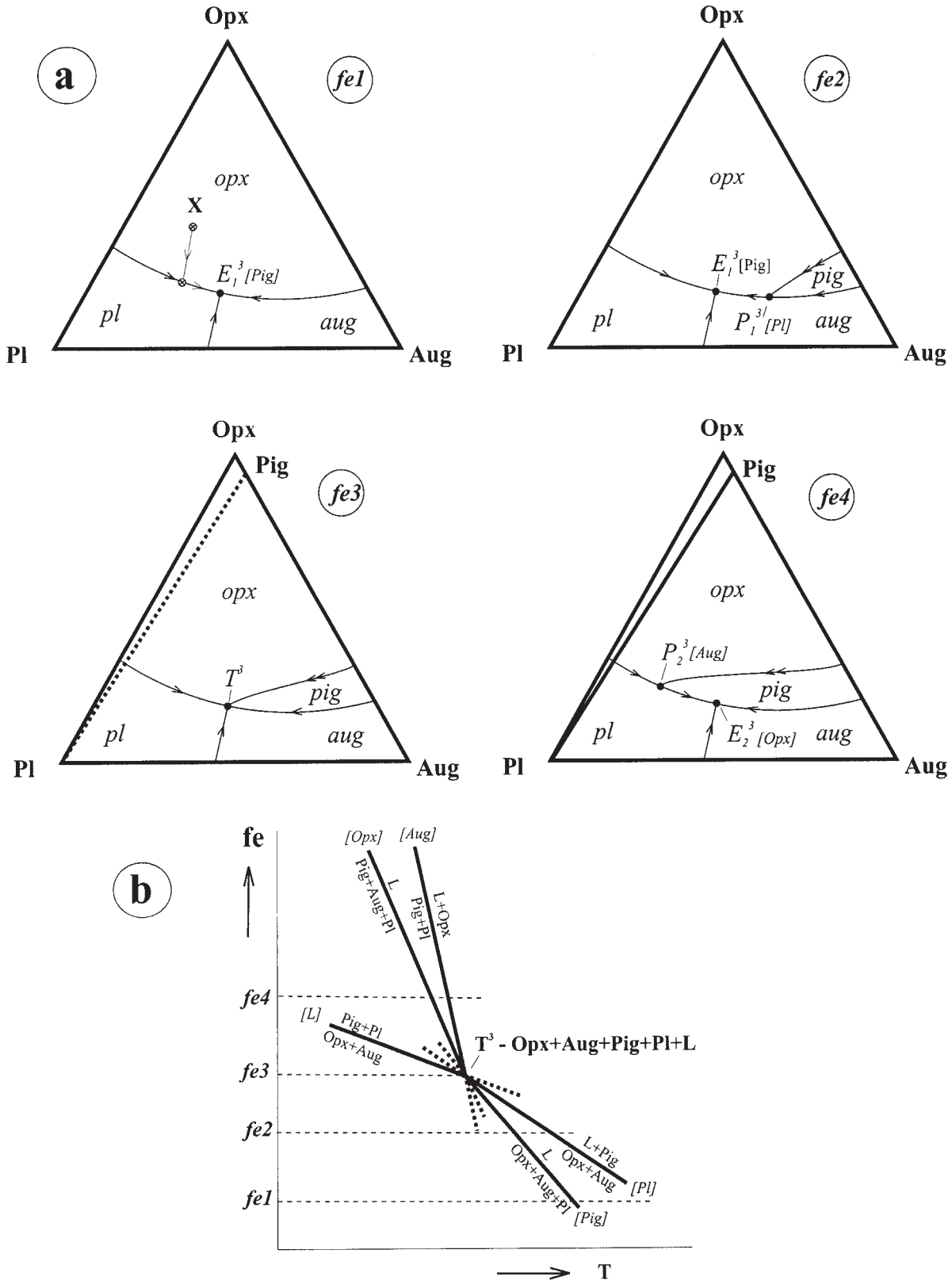

FIGURE 7. Projections of the upper part of the isobaric–isoplethic section $Ol^{25\text{-}50}$-Aug-Pl^{60}-Qtz onto the plane Opx-Aug-Pl (**a**), illustrating a hypothetical crystallization trend for the mafic melt X. The positions of the isobaric–isoplethic sections from *fe*1 to *fe*4 are represented by dotted lines in the *T-fe* isobaric projection (**b**). Brackets indicate phases that are absent in the equilibria.

field as differentiation progresses, will result in the liquid falling to the invariant point T^3 (Fig. 7, *fe*3). The three-pyroxene assemblage Opx + Aug + Pig + Pl is generated at this stage. With further expansion of the pigeonite volume, there is complete separation of the stability fields of orthopyroxene and augite (a new Alkemade line Pig-Pl forms). As a result, the liquid finds itself at a new eutectic point E_2^3 (Fig. 7, *fe*4), where the orthopyroxene-free mineral assemblage Aug + Pig + Pl will crystallize. Thus, the overall order of phase appearance is consistent with the typical pyroxene crystallization sequence for mafic layered intrusions, namely: Opx + Aug + Pl → Opx + Aug + Pig + Pl → Aug + Pig + Pl.

ACKNOWLEDGMENTS

John Longhi read an early version of the manuscript, and his insightful comments are gratefully acknowledged. We also thank H.Y. Yang, Don R. Baker, and B.R. Frost for their constructive reviews of the paper. Editing by Autumn Ford and Stacy Saari led to significant improvement in the wording of the text. We thank James Blencoe for his editorial input. The research was supported by grants from Thule Institute of the University of Oulu, and the Center for International Mobily (CIMO, Helsinki), which were awarded to R. M. Latypov.

REFERENCES CITED

Dubrovskii, M.I. (1998) Differentiation Trends of the Standard Alkalinity Olivine-normative Magmas and Corresponding Rock Series, 336 p. Apatity, Kola Science Center. (in Russian).

Eales, H.V. and Cawthorn, R.G. (1996) The Bushveld Complex. In R.G. Cawthorn, Ed., Layered intrusions, Developments in Petrology 15, p. 181–229. Elsevier, Amsterdam, The Netherlands.

Ehlers, E.G. (1972) The Interpretation of Geological Phase Diagrams, 280 p. W. H. Freeman, San Francisco.

Grove, T.L., Gerlach, D.C., and Sando, T.W. (1982) Origin of calc-alkaline series lavas at Medicine Lake volcano by fractionation, assimilation and mixing. Contributions to Mineralogy and Petrology, 80, 160–182

Grove, T.L., Gerlach, D.C., and Sando, T.W. (1983) Origin of calc-alkaline series lavas at Medicine Lake volcano by fractionation, assimilation and mixing: corrections and clarifications. Contributions to Mineralogy and Petrology, 82, 407–408

Grove, T.L. and Juster, T.C. (1989) Experimental investigations of low-Ca pyroxene stability and olivine-pyroxene-liquid equilibria at 1 atm in natural basaltic and andesitic liquids. Contributions to Mineralogy and Petrology, 103, 287–305.

Hess, H.H. (1941) Pyroxenes of common mafic magmas. Part 2. American Mineralogist, 26, 573–594.

Huebner, J.S. and Turnock, A.C. (1980) The melting relations at 1 bar of pyroxenes composed largely of Ca-, Mg-, and Fe-bearing components. American Mineralogist, 65, 225–271.

Korzhinskii, D.S. (1959) Physicochemical basis for analysis of the paragenesis of mineral, 142 p. New York, Consultants Bureau Inc.

Kozlov, E.K. (1973) Natural series of nickel-bearing intrusion rocks and their metallogeny, 288 p. Leningrad, Nauka (in Russian).

Latypov, R.M. and Chistyakova, S.Yu. (2001) Physical-chemical aspects of origin of the magnetite gabbro in the West-Pansky Tundra layered intrusion, Kola Peninsula, Russia. Petrology, 9, 1–23.

Longhi, J. (1987) Liquidus equilibria and solid solution in the system Anorthite-Forsterite-Wollastonite-Silica at low pressure. American Journal of Science, 287, 265–331.

Longhi, J. (1991) Comparative liquidus equilibria of hypersthene-normative basalts at low pressure. American Mineralogist, 76, 785–800.

Longhi, J. and Pan, V. (1988) A reconnaissance study of phase boundaries in low-alkali basaltic liquids. Journal of Petrology, 29, 115–147.

Nakamura, Y. and Kushiro I. (1970) Compositional relations of coexisting orthopyroxene, pigeonite and augite in a tholeiitic andesite from Hakone volcano. Contributions to Mineralogy and Petrology, 26, 265–275.

Odinets, A.Yu. (1971) Petrology of the Pana basic rock massif (Kola Peninsula), 186 p. Unpublished Ph.D. dissertation, Kola Science Center, Apatity (in Russian).

Ricci, J.E. (1951) The Phase Rule and Heterogeneous Equilibrium, 505 p. Toronto, D. Van Nostrand Company.

Schreinemakers, F.A. (1965) Papers by F.A. Schreinemakers, 1, 2. (1912–1925), 579 p. Pennsylvania, Pennsylvania State University.

Shi, P. and Libourel, G. (1991) The effects of FeO on the system CMAS at low pressure and implications for basalt crystallization processes. Contributions to Mineralogy and Petrology, 108, 129–145.

Von Gruenewaldt, G. (1970) On the phase change orthopyroxene-pigeonite and the resulting texture in the main and upper zone of the Bushveld complex in the eastern Transvaal. The Geological Society of South Africa, Special Publication 1, Department of Geology, University of Pretoria, South Africa, 67–73.

Wager, L.R. and Brown, G.M. (1968) Layered Igneous Rocks, 588 p. Edinburg and London, Oliver and Boyd.

Yang, H.Y. (1973) Crystallization of iron-free pigeonite in the system anorthite-diopside-enstatite-silica at atmospheric pressure. American Journal of Science, 273, 488–497.

MANUSCRIPT RECEIVED APRIL 26, 2000
MANUSCRIPT ACCEPTED DECEMBER 12, 2000
MANUSCRIPT HANDLED BY JAMES G. BLENCOE